

Report of Investigation: LA-ICPMS

Prepared by: Dr. Darin Schwartz; darinschwartz@boisestate.edu

Prepared for: Dr. Matt Morgan; Colorado Geological Survey

Table 1: Analytical Summary

Sample	N	n	MDA Candidates ¹		Modes			
			youngest date	youngest population	principal	2	3	4
BRDZ1	139	125	60.2 ± 4.1 Ma	67.1 ± 1.4 Ma (n=31; MSWD=0.91)	66.7 Ma	75 Ma	101.2 Ma	87.9 Ma
BRDZ3	139	129	72.8 ± 2.7 Ma	76.4 ± 1.7 Ma (n=9; MSWD=0.75)	93.8 Ma	1720.6 Ma	1621.7 Ma	585.2 Ma
KH344	140	135	63.5 ± 3.9 Ma	1726 ± 22.3 Ma (n=134; MSWD=0.86)	1708.2 Ma	1509 Ma	63.5 Ma	
LL65	117	97	70.1 ± 2.3 Ma	70.9 ± 1.5 Ma (n=2; MSWD=0.6)	1705.4 Ma	1407.3 Ma	155.5 Ma	1083.9 Ma
WS027DZ	121	102	27.5 ± 1.4 Ma	96.7 ± 2 Ma (n=4; MSWD=0.47)	1435.8 Ma	1735.8 Ma	92 Ma	1042.5 Ma

MDA = maximum depositional age; N = total number of analyses; n = number of concordant analyses

¹ uncertainties reported at 95% confidence

Analyst's Comments

Of the five samples submitted for detrital zircon analysis, all yielded abundant zircons from crushing and mineral separation procedures.

All samples but KH344 produced Late Cretaceous maximum depositional ages based upon significant numbers of young grains. Of note, however, a single youngest grain from sample KH344 also produced a Late Cretaceous age and a single Oligocene age grain was recovered from WS027DZ. In general, the proportion of Cretaceous and older grains is variable between samples. Specifically, BRDZ1 contained a majority Cretaceous ages, while the other samples have more dominant Paleozoic populations.

Analytical Methods

The analytical methods summarized below apply to samples listed in Table 1.

Sample Preparation

An abundant population of relatively small, (approximately 50-200 micron in long dimension), angular to rounded zircon crystals was separated from the provided hand samples by conventional density and magnetic methods. The entire zircon separate was placed in a muffle furnace at 900°C for 60 hours in quartz beakers to anneal minor radiation damage; annealing enhances cathodoluminescence emission (Nasdala et al., 2002), promotes more reproducible inter-element fractionation during laser ablation inductively coupled plasma mass spectrometry (LA-ICPMS) (Allen and Campbell, 2012), and prepares the crystals for any subsequent chemical abrasion (Mattinson, 2005). Following annealing, individual grains for each sample were sieved into three size fractions (<70 micron, 70-150 micron and >150 micron) and mounted with other samples by size fraction, using 0.5 mm aperture strips of double-sided tape, secured in epoxy. Grain mounts were ground to expose the interiors of zircon crystals, polished with 0.3 micron alumina, and imaged by cathodoluminescence (CL) on a scanning electron microscope. Laser spots were placed on random swaths of grains from multiple rows for each size fraction, proportional to the mass fraction of zircons from each size, typically 4 grains in the >150 micron fraction, 28 grains in the 70-150 micron fraction and 112 in <70 micron fraction. Laser spots were placed on the most volumetrically dominant growth domains for each grain, in locations devoid of apparent cracks and inclusions as interpreted from CL zonation patterns and transmitted/reflected light imagery.

LA-ICPMS analysis

LA-ICPMS analysis utilized a ThermoFisher iCAP RQ quadrupole inductively coupled plasma mass spectrometer coupled to a Teledyne Analyte Excite+ 193 nm excimer laser ablation system. In-house analytical protocols, standard materials, and data reduction software were used for acquisition and calibration of U and Pb isotope ratios dates and a suite of high field strength elements (HFSE), and rare earth elements (REE), and titanium elemental concentrations. Zircon grains were ablated with a laser spot diameter of 20 μm using fluence and pulse rates of $\sim 2.5 \text{ J/cm}^2$ and 5 Hz, during a 45 second analysis (15 sec gas blank, 20 sec ablation, and 10 sec washout) that excavated a pit $\sim 7 \mu\text{m}$ deep. Ablated material was carried by a combined 1.2 L/min He gas stream from the two-volume ablation cell to the nebulizer flow of the plasma. Quadrupole dwell times were 5 ms for Si and Zr, 200 ms for ^{49}Ti and ^{207}Pb , 80 ms for ^{206}Pb , 40 ms for ^{202}Hg , ^{204}Pb , ^{208}Pb , ^{232}Th , and ^{238}U and 10 ms for all other HFSE and REE; total sweep duration is 950 ms. Background count rates for each analyte were obtained prior to each spot analysis and subtracted from the raw count rate for each analyte. For concentration calculations, background-subtracted count rates for analytes were internally normalized to ^{29}Si and calibrated with respect to NIST SRM-610 and -612 glasses as the primary concentration standards. Analyses compromised by glass or mineral inclusions were identified based on selected elemental signal excursions, for example Ti and P, and associated sweeps were generally discarded. U-Pb dates from these analyses are considered valid if the U-Pb ratios appear to have been unaffected by the inclusions. Signals at mass 204 were normally indistinguishable from zero following subtraction of mercury backgrounds measured during the gas blank ($<100 \text{ cps } ^{202}\text{Hg}$), and thus dates are reported without common Pb correction. Rare sweeps or whole analyses with mass 204 signals above background were rejected.

U-Pb and Pb-Pb dates are corrected for instrumental fractionation using background-subtracted ratios and are calibrated with respect to interspersed measurements of zircon standards and reference materials. The primary zircon standard Plešovice zircon (Sláma et al., 2008) is used to monitor time-dependent instrumental fractionation based on two analyses for every 14 analyses of unknown zircon. A polynomial fit to the primary standard analyses versus time yields each spot-specific fractionation factor and its standard deviation.

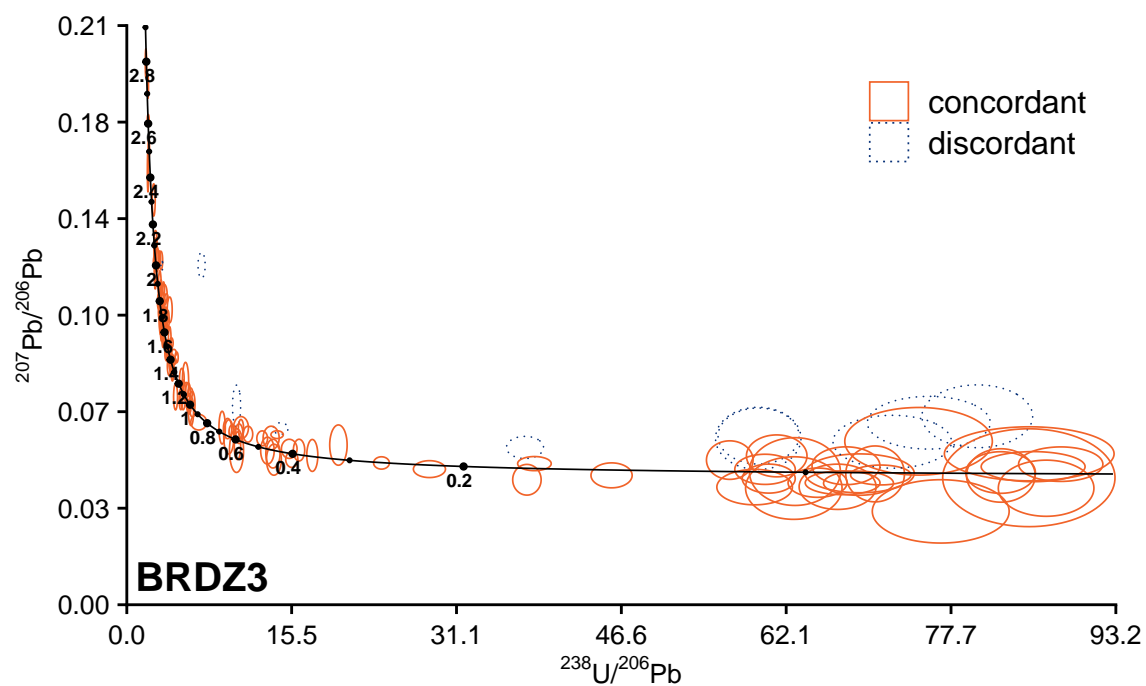
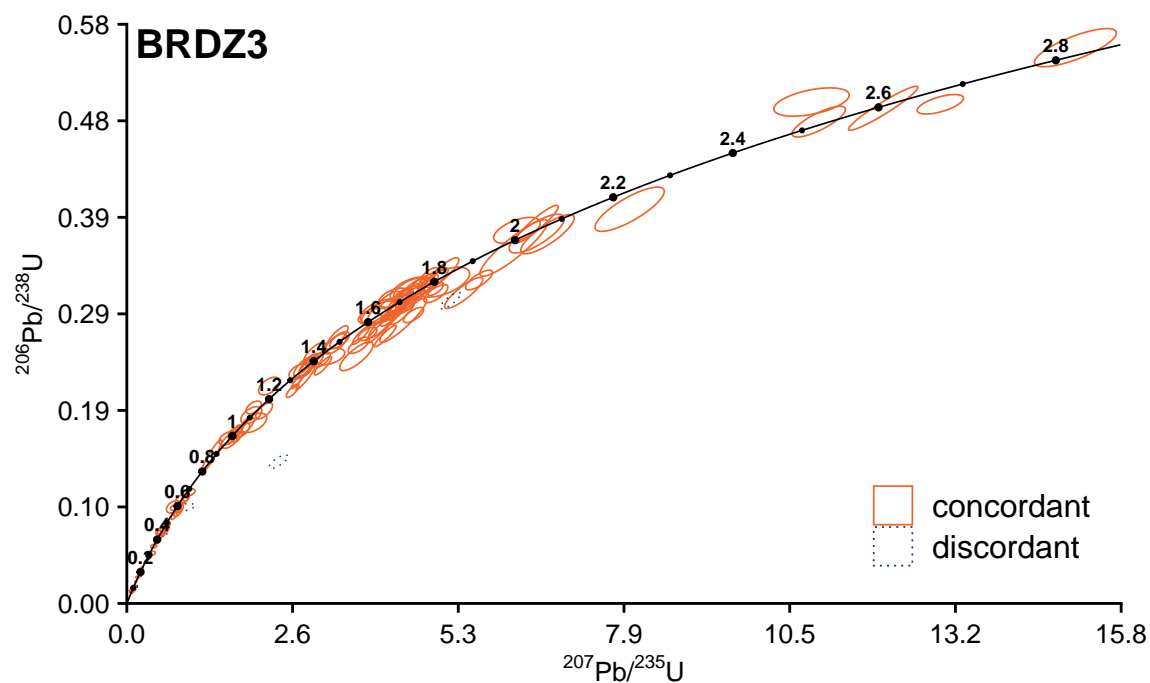
tion. A secondary bias correction is subsequently applied to unknowns on the basis of the residual age bias as a function of radiogenic Pb count rate in standard materials including Seiland, Zirconia, and Plešovice, FC1 and 91500. Error contributions from counting statistics and background subtraction are propagated into the analytical uncertainties for isotope ratios and U-Pb dates. Following the recommendations of Horstwood et al. (2016) the uncertainties on each date are reported with and without systematic uncertainties from the primary reference material calibration. Additional details of methodology and reproducibility are reported in Rivera et al. (2013) and Macdonald et al. (2018).

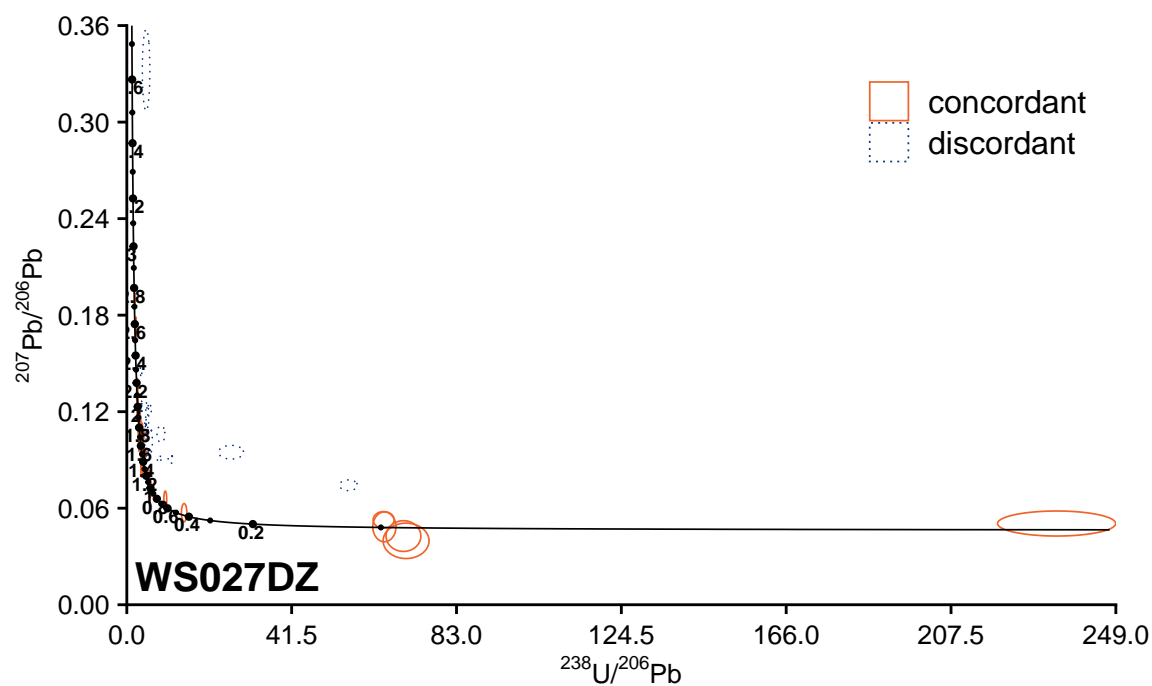
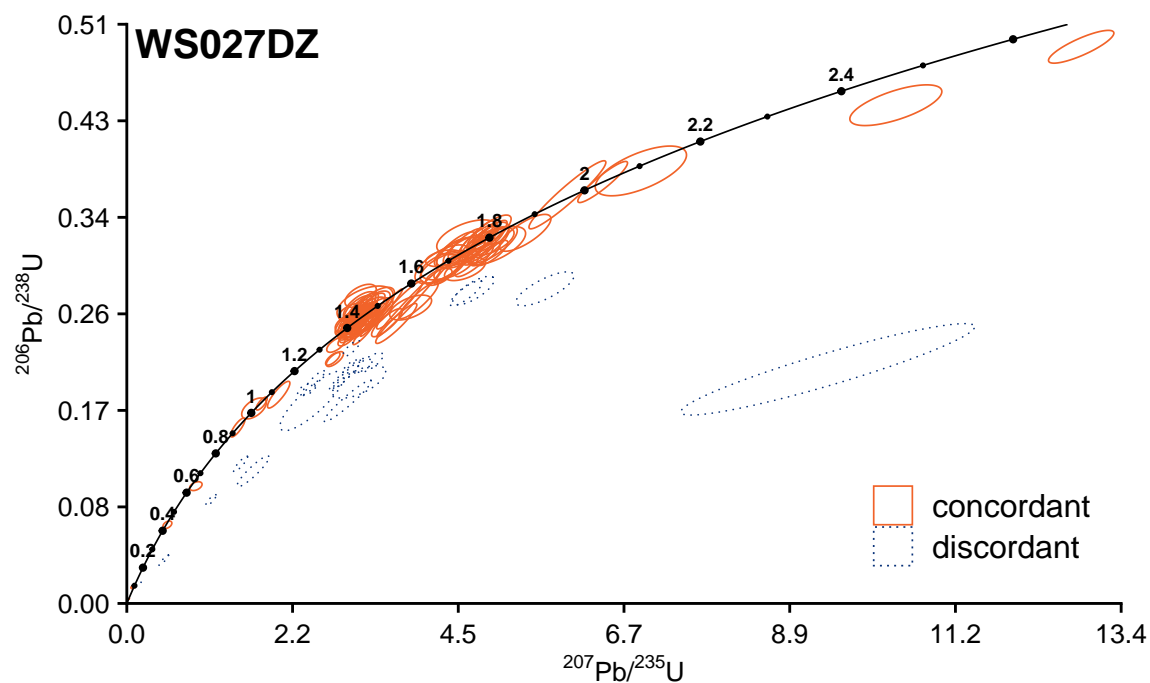
Calculations used in analytical summary

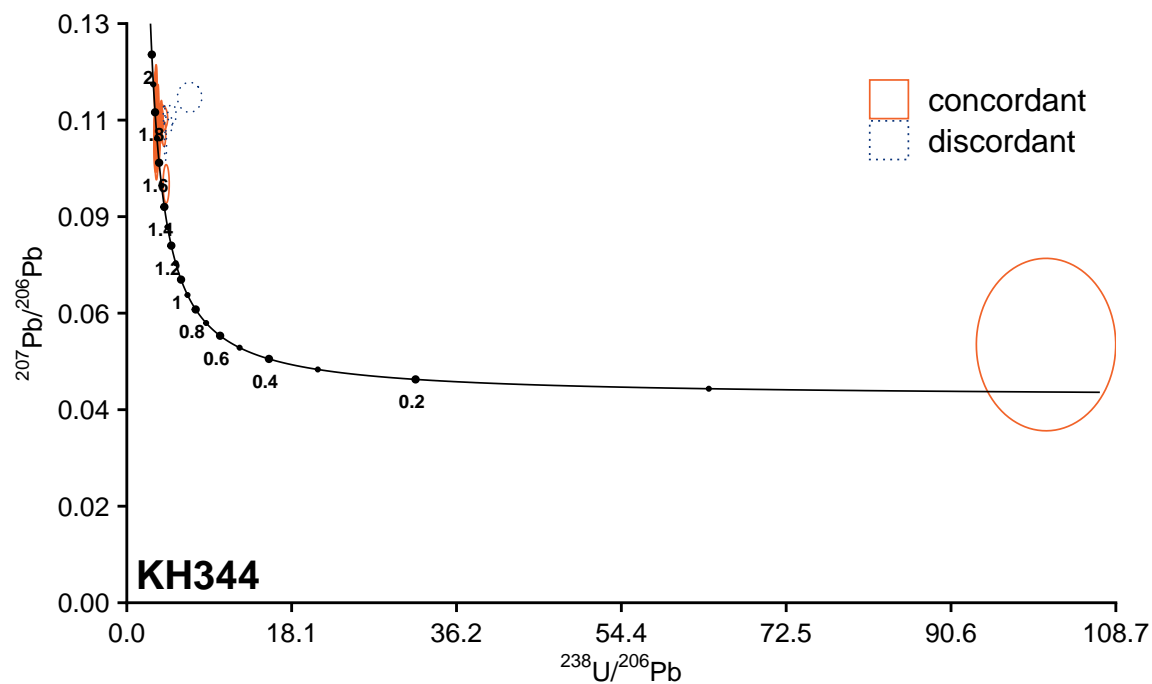
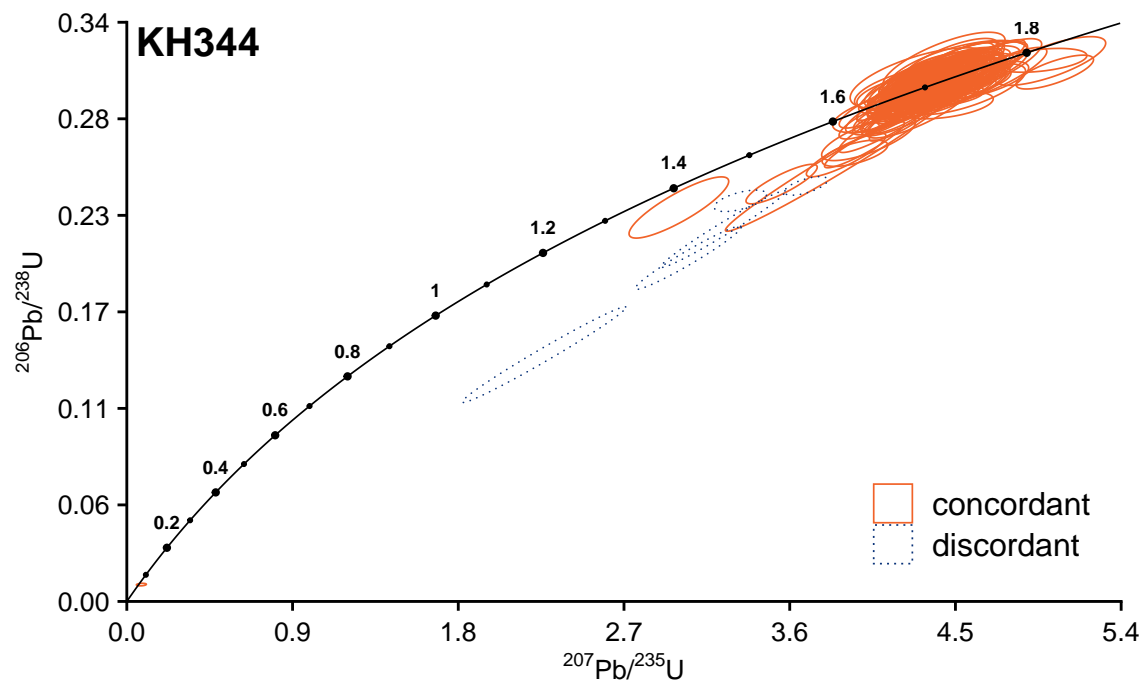
The independent decay chains of ^{238}U to ^{206}Pb and ^{235}U to ^{207}Pb provide a closed-system, or concordance, check via agreement between dates calculated from each U-Pb decay scheme (Wetherill, 1956; Tera and Wasserburg, 1972; Schoene, 2014). Concordance is a primary criteria for addressing the interpretive age accuracy of an analysis, and can be calculated via a number of metrics (e.g., Ludwig, 1998; Vermeesch, 2020), but is most often expressed as the relative difference between the $^{207}\text{Pb}/^{206}\text{Pb}$ and $^{206}\text{Pb}/^{238}\text{U}$ ratios (or dates), or the $^{207}\text{Pb}/^{235}\text{U}$ and $^{206}\text{Pb}/^{238}\text{U}$ ratios (or dates). While $^{207}\text{Pb}/^{206}\text{Pb}$ - $^{206}\text{Pb}/^{238}\text{U}$ concordancy is robust for Precambrian zircon dates, it deteriorates for Phanerozoic dates due to the increased linearity of the Phanerozoic concordia curve and corresponding highly oblique intersection of discordia lines. By contrast, $^{207}\text{Pb}/^{235}\text{U}$ - $^{206}\text{Pb}/^{238}\text{U}$ concordancy is robust regardless of absolute age. The total number of analyses (N) and the number of concordant analyses (n) are listed in Table 1. We define concordant analyses (n) as those with $^{206}\text{Pb}/^{238}\text{U}$ and $^{207}\text{Pb}/^{235}\text{U}$ dates that are within 5% of agreement, assessed within the 95% confidence interval of the propagated error in discordance (Gibson et al., 2021). Concordant and discordant analyses for each sample are plotted in the Wetherill and Tera-Wasserburg concordia plots section of this report. Analyses for zircon standards in each experiment (analytical session) are similarly plotted on Wetherill concordia plots at the end of this report.

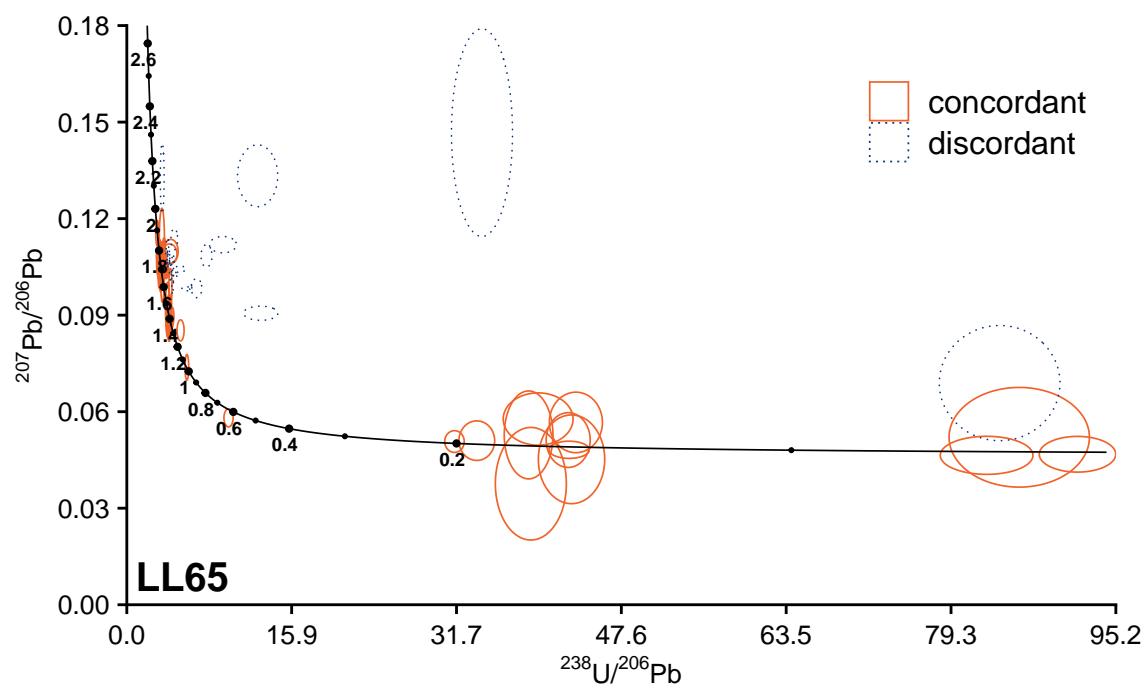
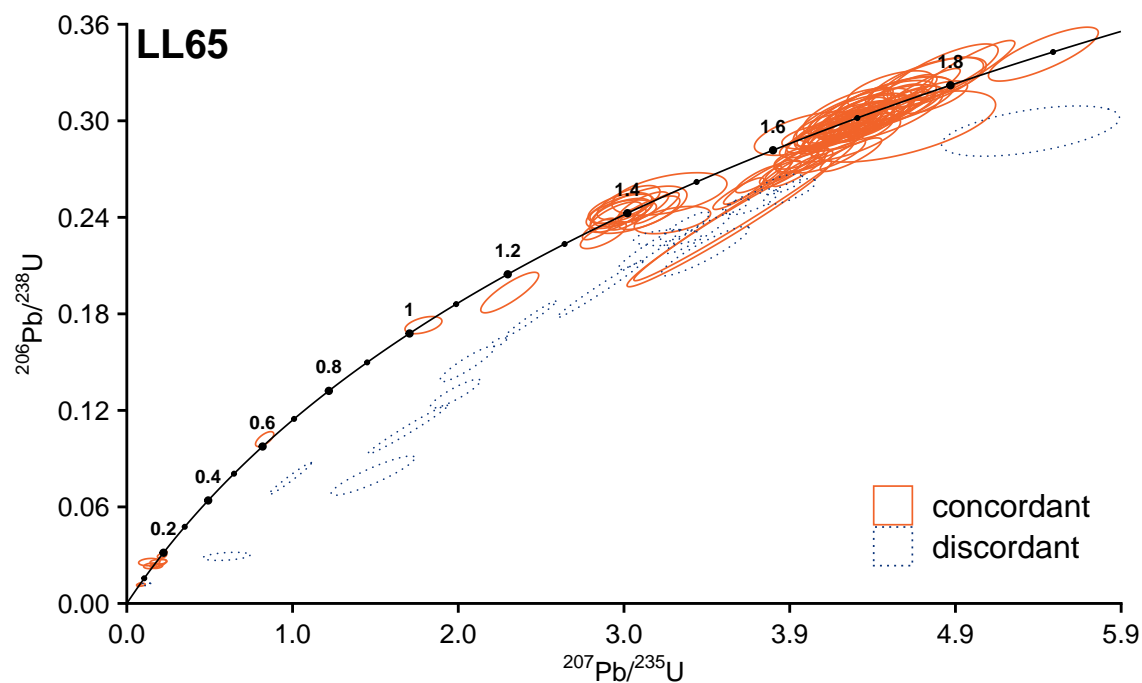
A maximum depositional age (MDA) for sedimentary rocks may be assessed using a variety of methods (Vermeesch, 2021). The two MDA candidates presented in Table 1 are the youngest single concordant analysis (youngest date) and its 2-sigma uncertainty, and the weighted mean of the youngest group of dates ($n > 2$) that together yield an MSWD < 1 (Wendt and Carl, 1991), and full 95% confidence interval for the weighted mean of this population. This approach is based on the recommendations of Herriott et al. (2019) established by comparing MDA interpretations from high n LA-ICPMS datasets to MDA interpretations obtained from more accurate and precise CA-IDTIMS method on the same zircon grains. However, it is important to consider that each of these MDA candidates, or an MDA obtained from another approach, should be assessed on a case-by-case basis and grounded with geological context.

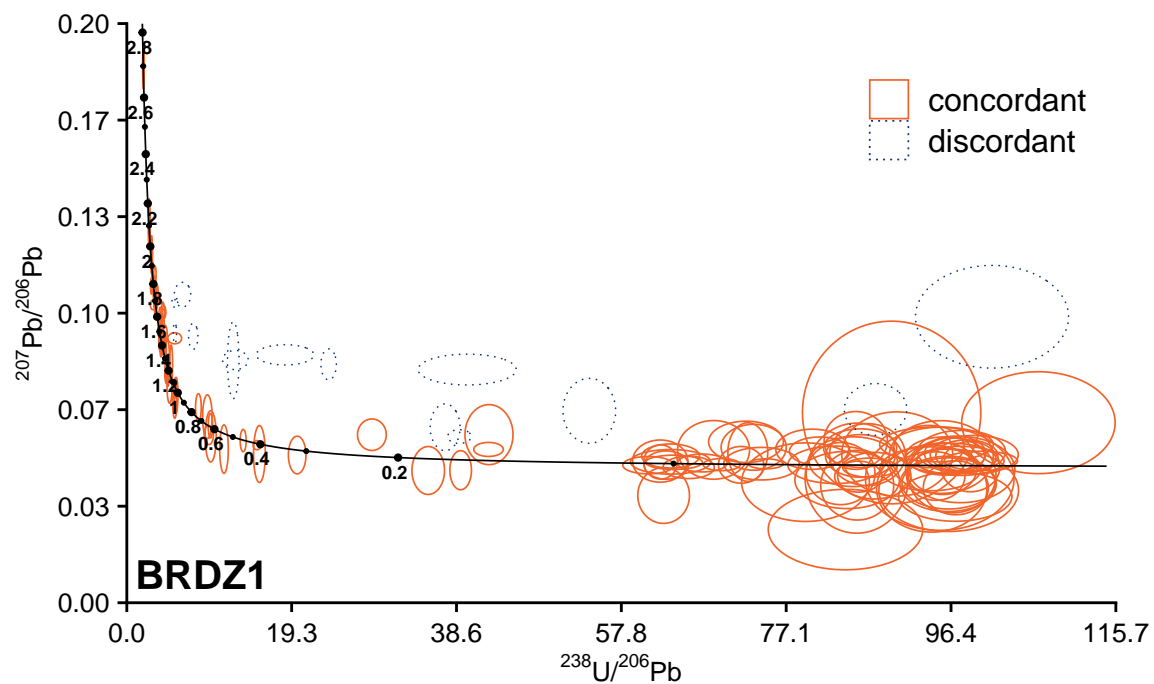
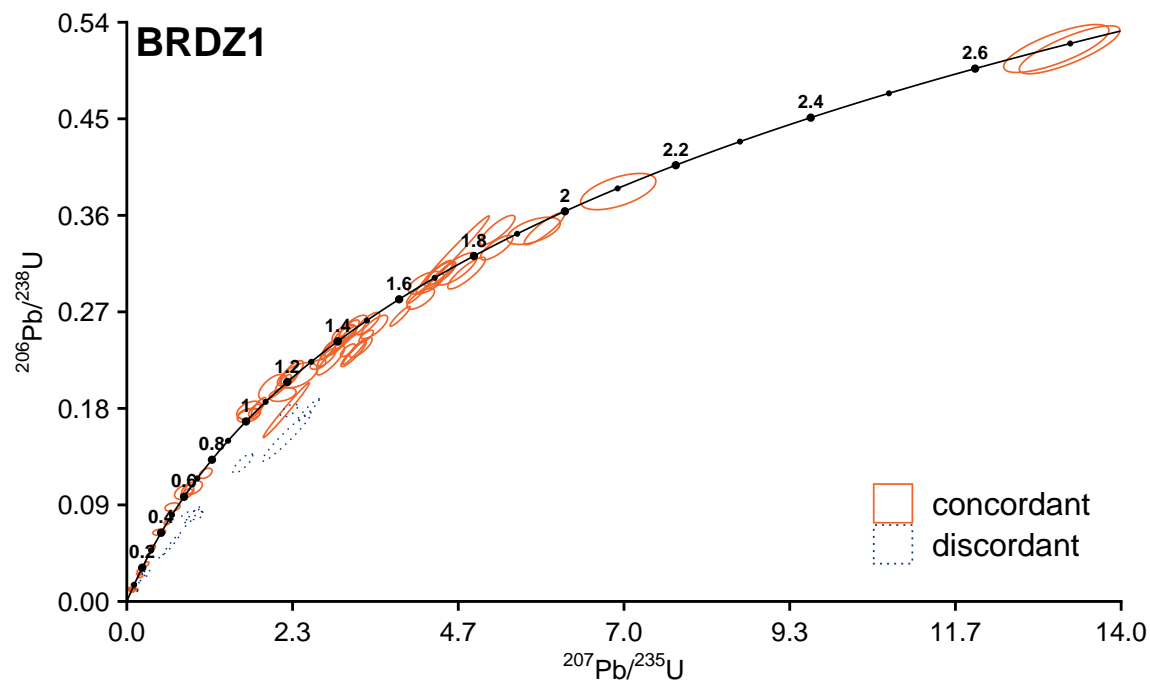
Kernel density estimators (KDEs) for each sample were constructed using functions from the IsoplotR package, employing an adaptive bandwidth (Vermeesch, 2018). The four most prominent modes in the KDE for each sample are listed in Table 1.

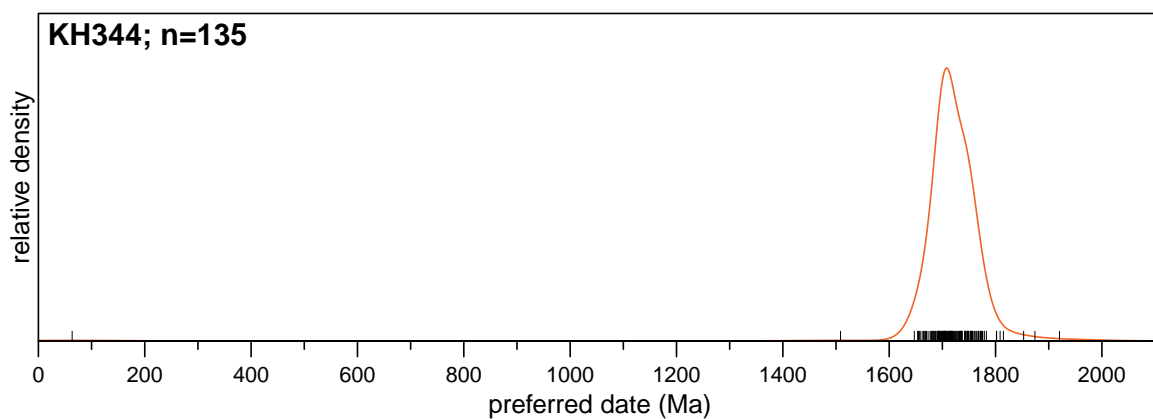
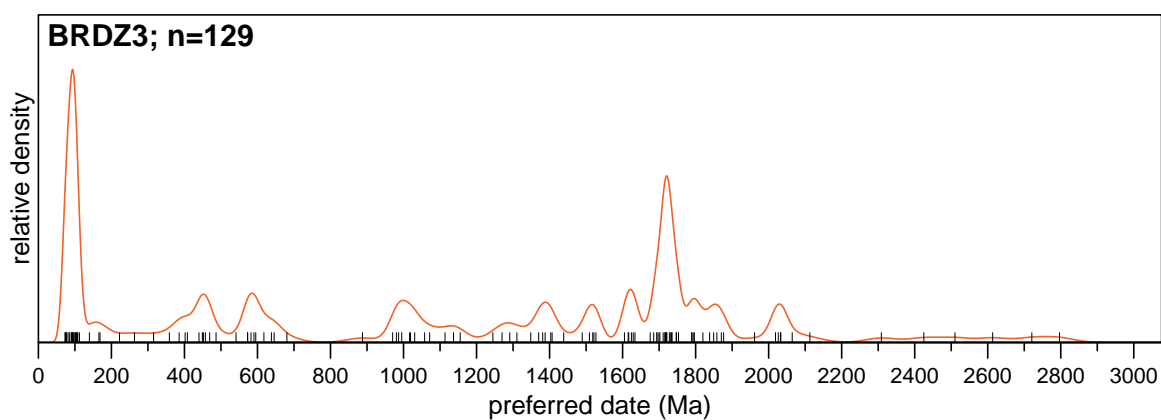
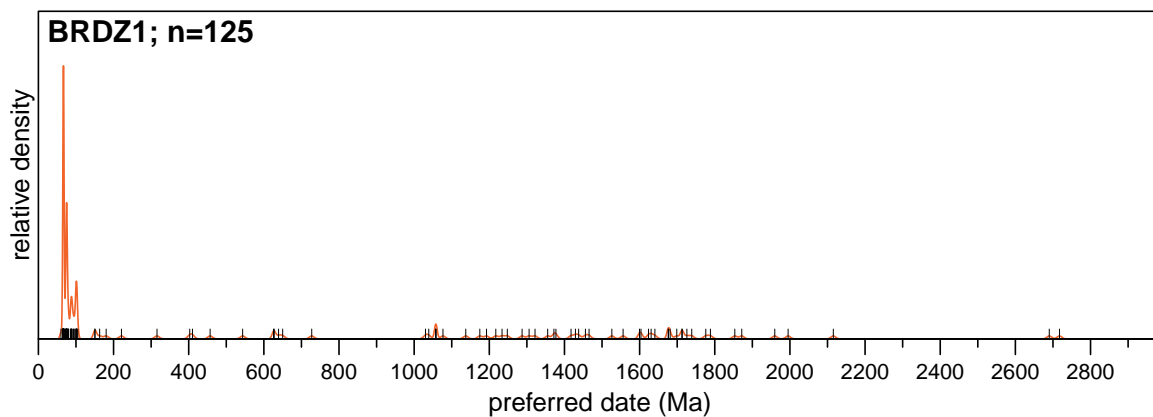


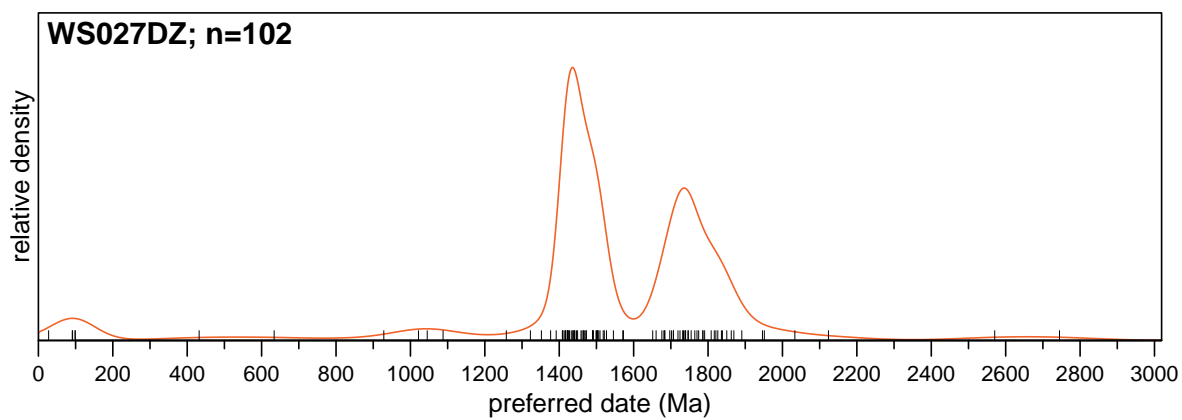
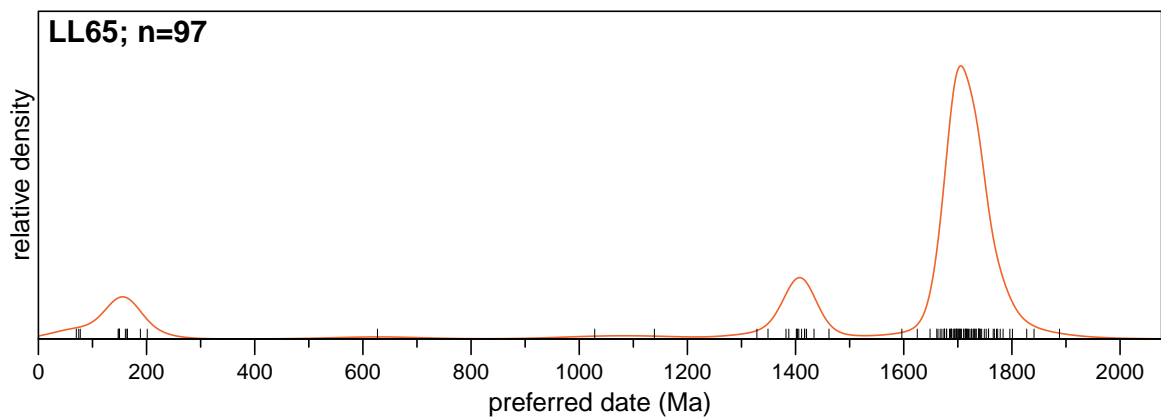




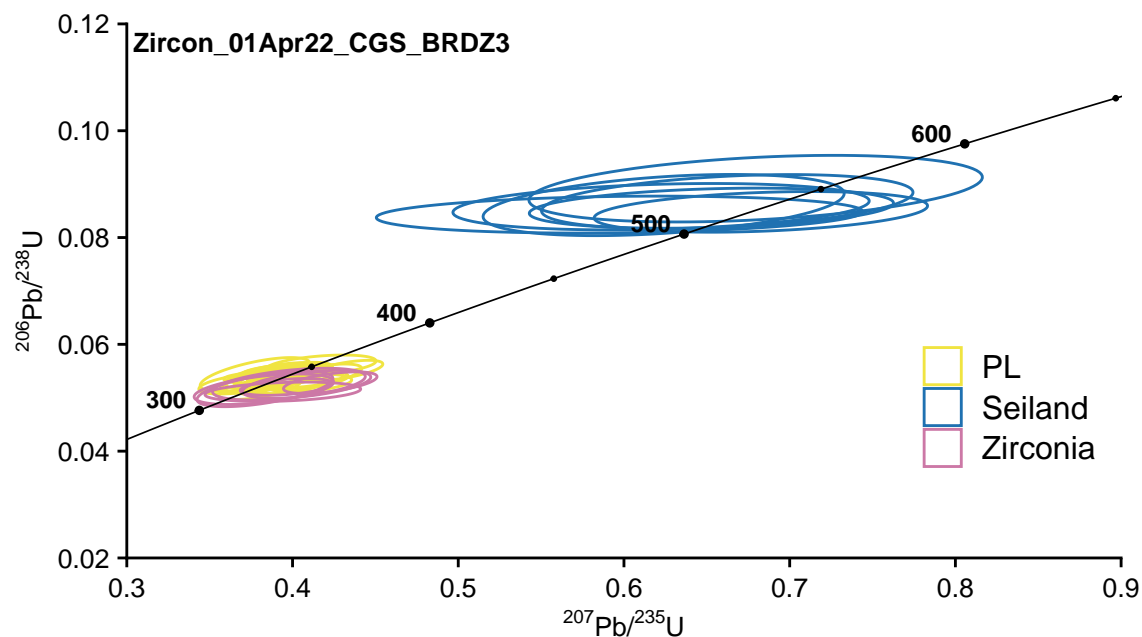
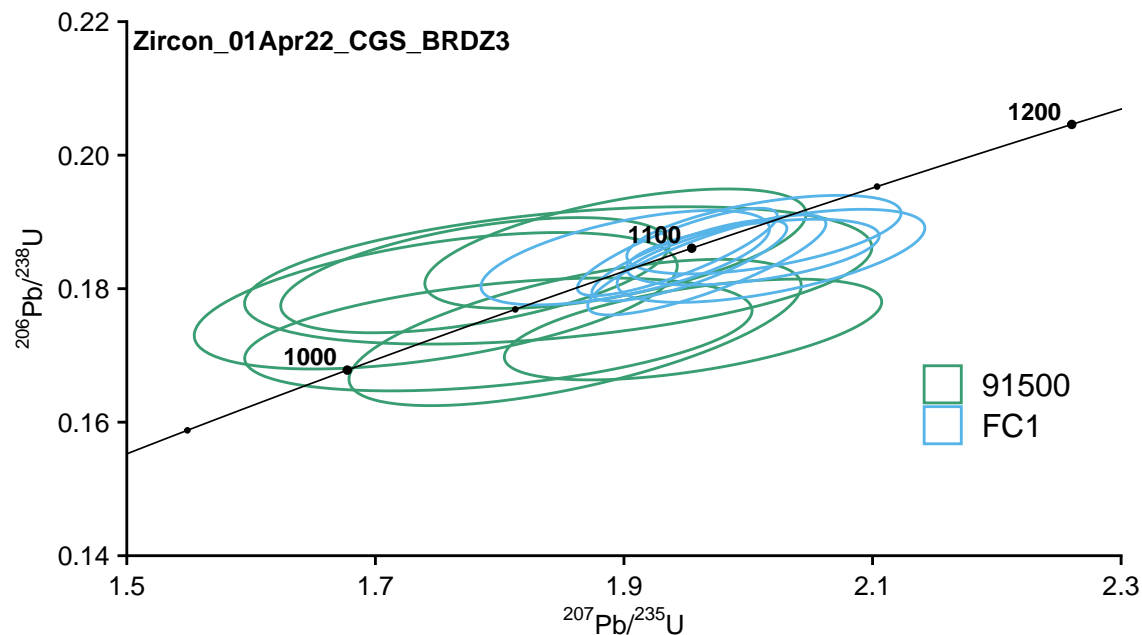


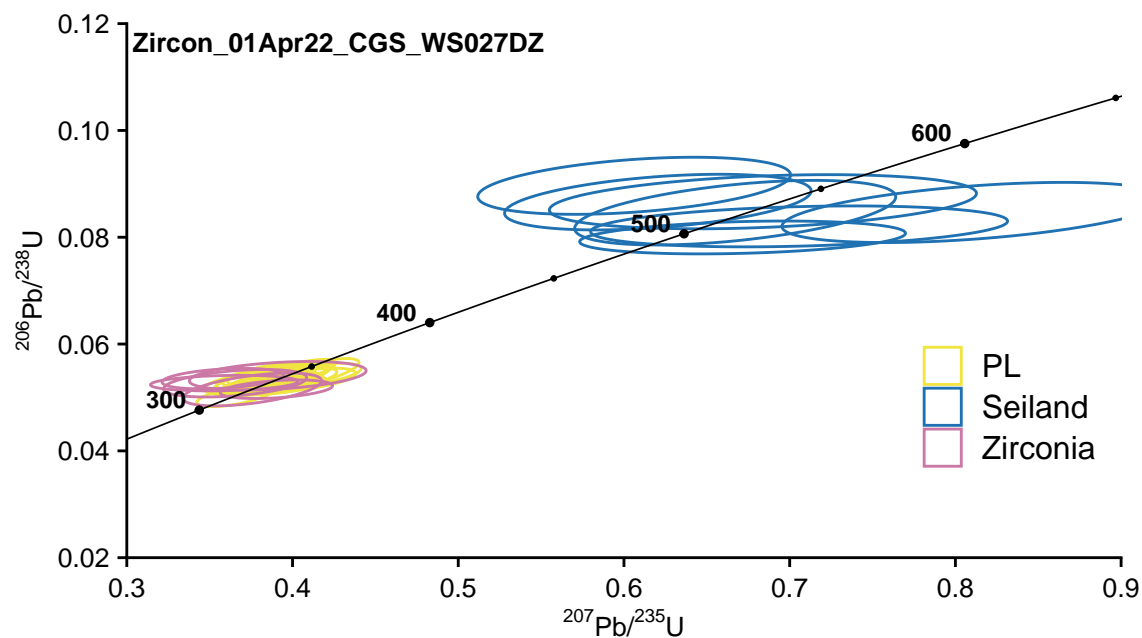
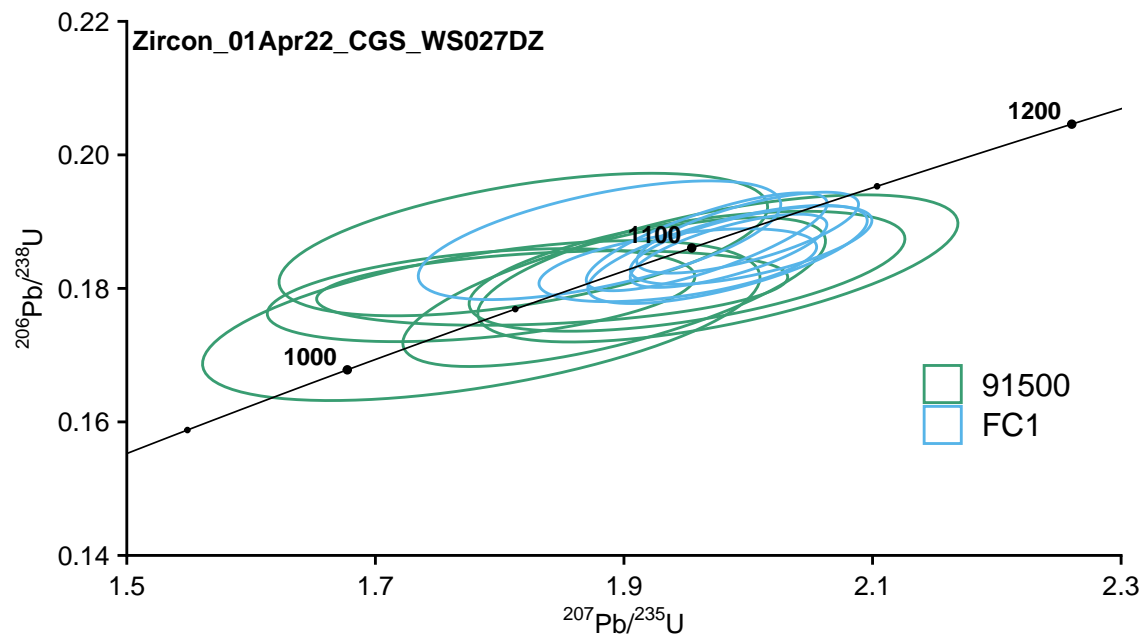


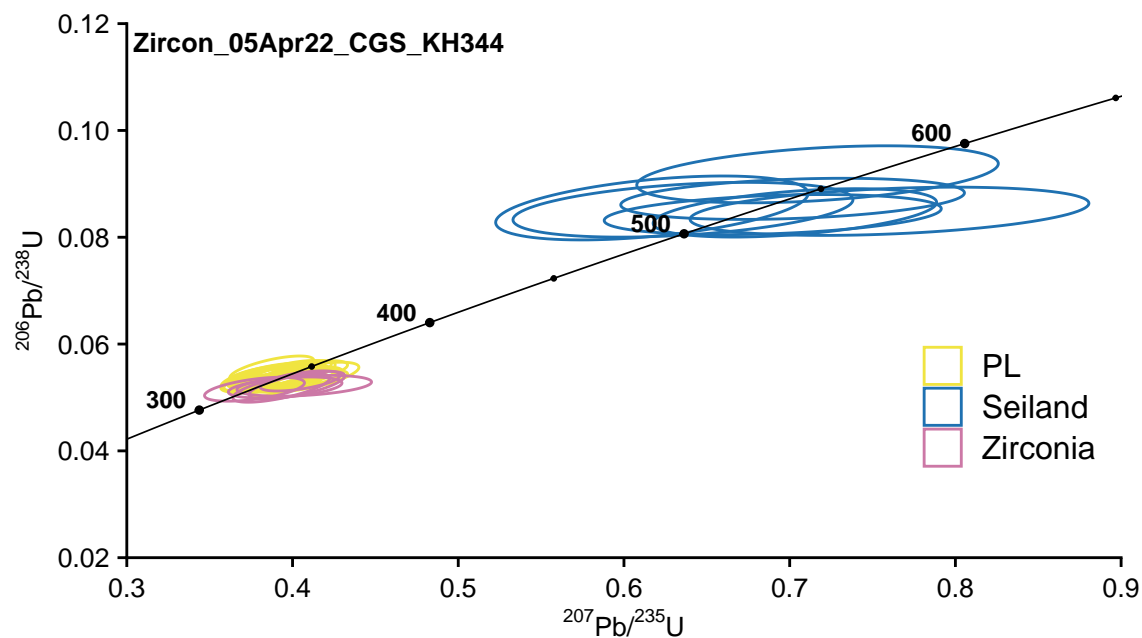
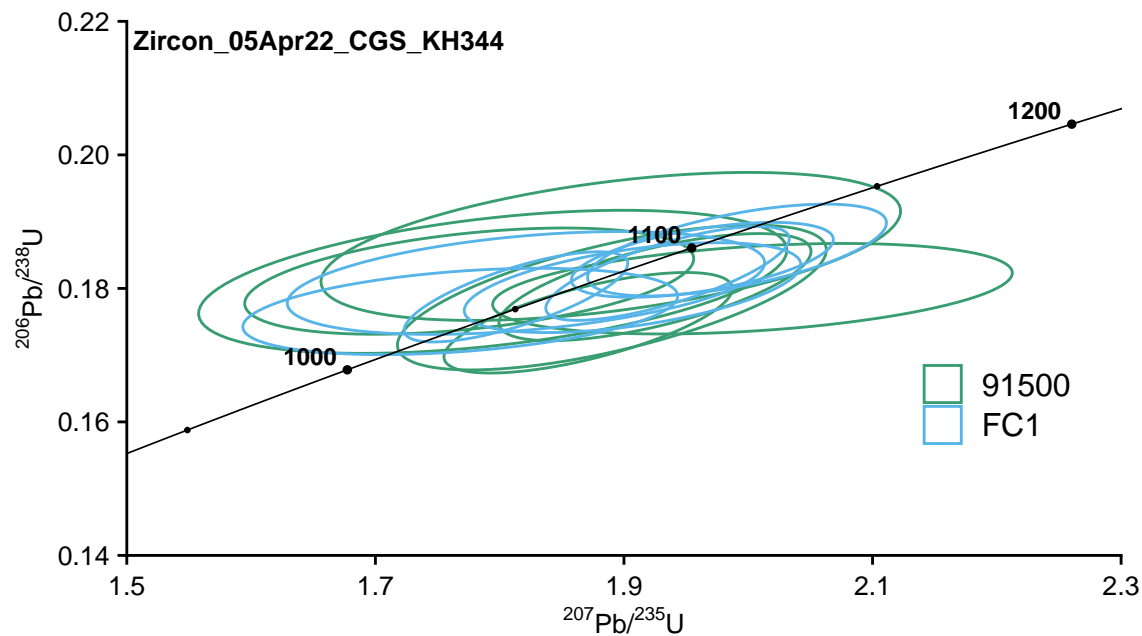


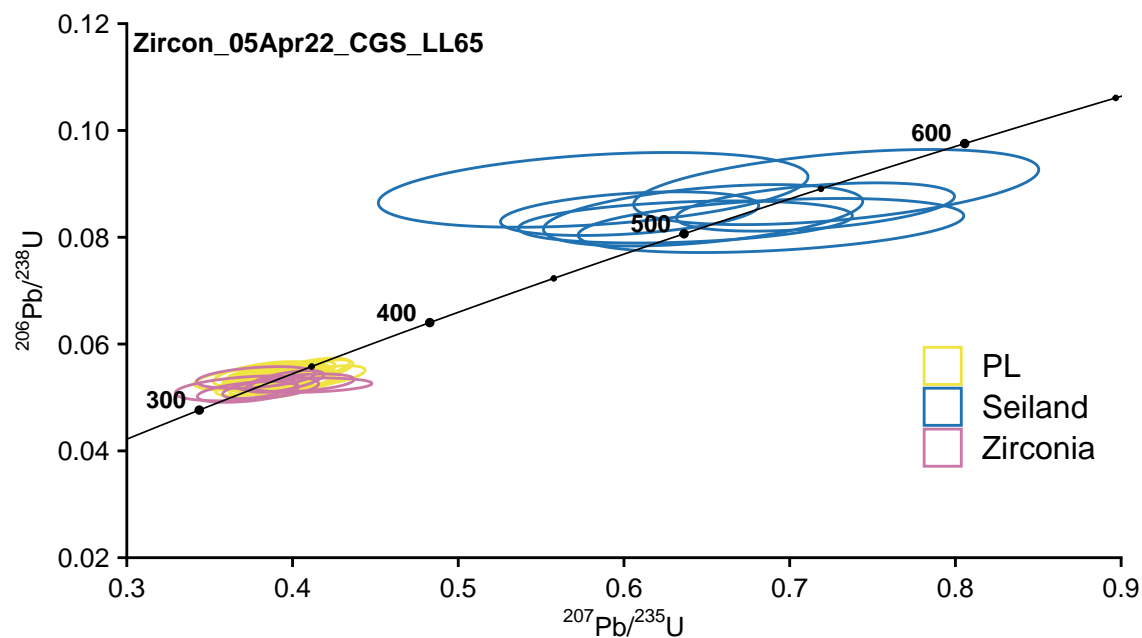
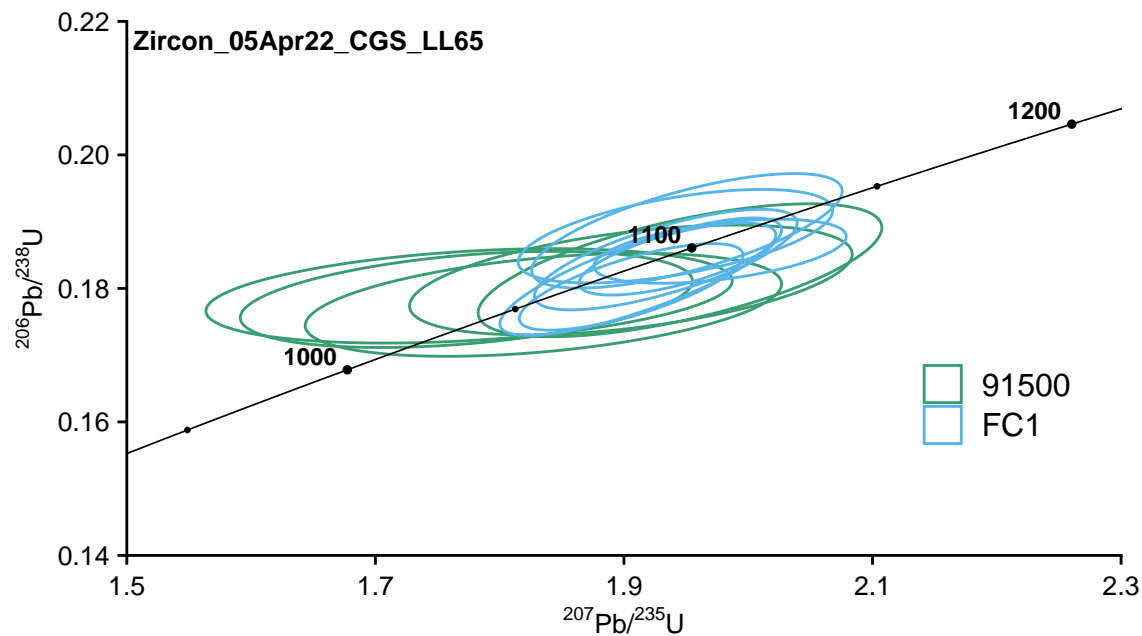


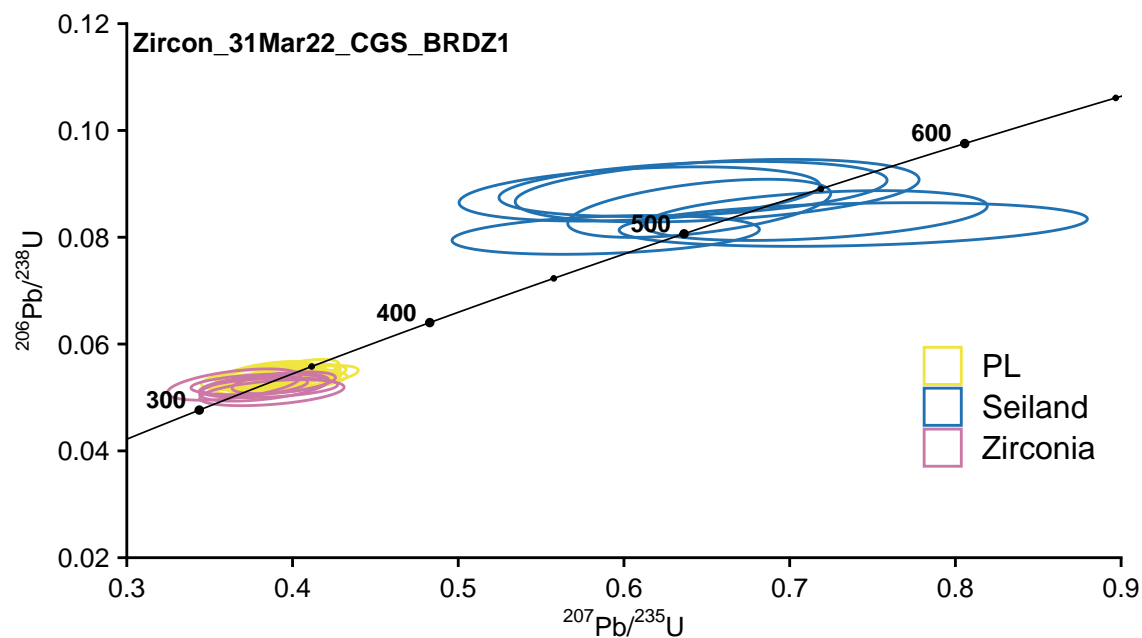
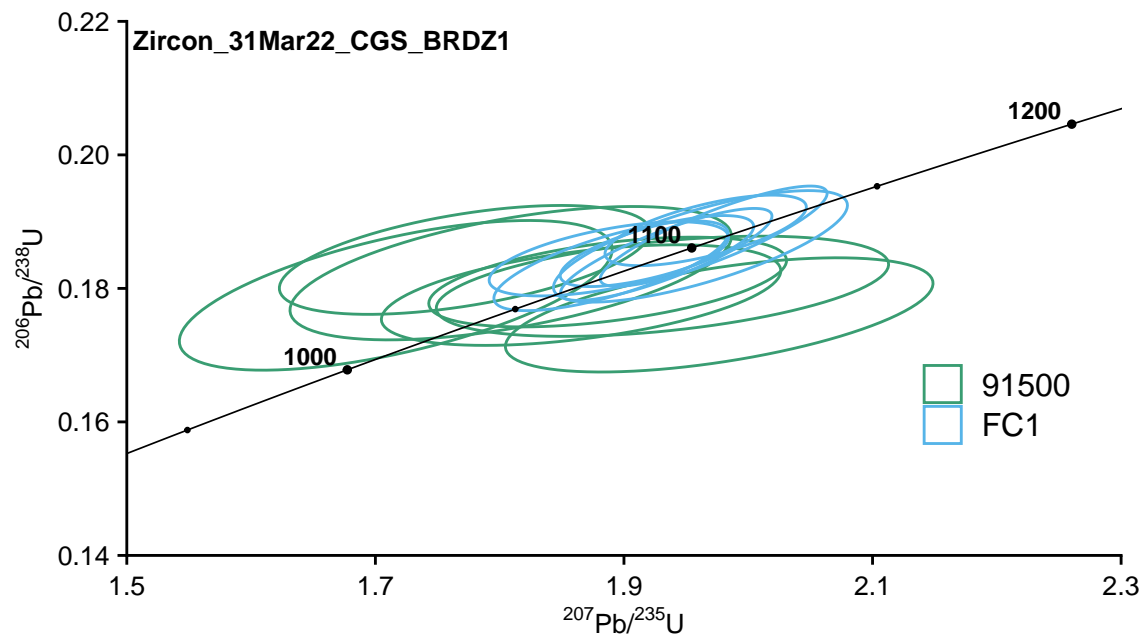
Wetherill concordia plots for standards (by analytical session)





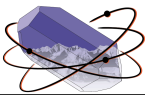






References

- Allen, Charlotte M., and Ian H. Campbell. 2012. "Identification and elimination of a matrix-induced systematic error in LA-ICP-MS 206Pb/238U dating of zircon." *Chemical Geology* 332: 157–65. <https://doi.org/10.1016/j.chemgeo.2012.09.038>.
- Gibson, Timothy M, Karol Faehnrich, James F Busch, William C McClelland, Mark D Schmitz, and Justin V Strauss. 2021. "A detrital zircon test of large-scale terrane displacement along the Arctic margin of North America." *Geology* 49 (5): 545–50. <https://doi.org/10.1130/g48336.1>.
- Herriott, Trystan M, James L Crowley, Mark D Schmitz, Marwan A Wartes, and Robert J Gillis. 2019. "Exploring the law of detrital zircon: LA-ICP-MS and CA-TIMS geochronology of Jurassic forearc strata, Cook Inlet, Alaska, USA." *Geology* 47 (11): 1044–48. <https://doi.org/10.1130/g46312.1>.
- Horstwood, Matthew S. A., Jan Košler, George Gehrels, Simon E. Jackson, Noah M. McLean, Chad Paton, Norman J. Pearson, et al. 2016. "Community-Derived Standards for LA-ICP-MS U-(Th)-Pb Geochronology – Uncertainty Propagation, Age Interpretation and Data Reporting." *Geostandards and Geoanalytical Research* 40 (3): 311–32. <https://doi.org/10.1111/j.1751-908x.2016.00379.x>.
- Ludwig, Kenneth R. 1998. "On the Treatment of Concordant Uranium-Lead Ages." *Geochimica Et Cosmochimica Acta* 62 (4): 665–76. [https://doi.org/10.1016/s0016-7037\(98\)00059-3](https://doi.org/10.1016/s0016-7037(98)00059-3).
- Macdonald, Francis A., Mark D. Schmitz, Justin V. Strauss, Galen P. Halverson, Timothy M. Gibson, Athena Eyster, Grant Cox, Peter Mamrol, and James L. Crowley. 2018. "Cryogenian of Yukon." *Precambrian Research* 319 (Bulletin 9 1997): 114–43. <https://doi.org/10.1016/j.precamres.2017.08.015>.
- Mattinson, James M. 2005. "Zircon U–Pb chemical abrasion ('CA-TIMS') method: Combined annealing and multi-step partial dissolution analysis for improved precision and accuracy of zircon ages." *Chemical Geology* 220 (1-2): 47–66. <https://doi.org/10.1016/j.chemgeo.2005.03.011>.
- Nasdala, Lutz, Christian L Lengauer, John M Hanchar, Andreas Kronz, Richard Wirth, Philippe Blanc, Allen K Kennedy, and Anne-Magali Seydoux-Guillaume. 2002. "Annealing radiation damage and the recovery of cathodoluminescence." *Chemical Geology* 191 (1-3): 121–40. [https://doi.org/10.1016/s0009-2541\(02\)00152-3](https://doi.org/10.1016/s0009-2541(02)00152-3).
- Rivera, Tiffany A., Michael Storey, Mark D. Schmitz, and James L. Crowley. 2013. "Age intercalibration of 40Ar/39Ar sanidine and chemically distinct U/Pb zircon populations from the Alder Creek Rhyolite Quaternary geochronology standard." *Chemical Geology* 345 (Earth and Planetary Science Letters 189 2001): 87–98. <https://doi.org/10.1016/j.chemgeo.2013.02.021>.
- Schmitz, Mark D., and Blair Schoene. 2007. "Derivation of isotope ratios, errors, and error correlations for U–Pb geochronology using 205Pb-235U-(233U)-spiked isotope dilution thermal ionization mass spectrometric data." *Geochemistry, Geophysics, Geosystems* 8 (8): n/a–. <https://doi.org/10.1029/2006gc001492>.
- Schoene, Blair. 2014. "U–Th–Pb Geochronology." *Treatise on Geochemistry 2nd Edition*, 341–78. <https://doi.org/10.1016/b978-0-08-095975-7.00310-7>.
- Sláma, Jiří, Jan Košler, Daniel J. Condon, James L. Crowley, Axel Gerdes, John M. Hanchar, Matthew S. A. Horstwood, et al. 2008. "Plešovice zircon — A new natural reference material for U–Pb and Hf isotopic microanalysis." *Chemical Geology* 249 (1-2): 1–35. <https://doi.org/10.1016/j.chemgeo.2007.11.005>.
- Spencer, Christopher J., Christopher L. Kirkland, and Richard J. M. Taylor. 2016. "Strategies towards statistically robust interpretations of in situ U–Pb zircon geochronology." *Geoscience Frontiers* 7 (4): 581–89. <https://doi.org/10.1016/j.gsf.2015.11.006>.
- Tera, Fouad, and G. J. Wasserburg. 1972. "U–Th–Pb systematics in three Apollo 14 basalts and the problem of initial Pb in lunar rocks." *Earth and Planetary Science Letters* 14 (3): 281–304. [https://doi.org/10.1016/0012-821x\(72\)90128-8](https://doi.org/10.1016/0012-821x(72)90128-8).
- Vermeesch, Pieter. 2018. "IsoplotR: a free and open toolbox for geochronology." *Geoscience Frontiers* 9 (5): 1479–93. <https://doi.org/10.1016/j.gsf.2018.04.001>.
- . 2020. "On the treatment of discordant detrital zircon U–Pb data." *Geochronology Discussions* 2020:



1–19. <https://doi.org/10.5194/gchron-2020-38>.

———. 2021. “Maximum depositional age estimation revisited.” *Geoscience Frontiers* 12 (2): 843–50. <https://doi.org/10.1016/j.gsf.2020.08.008>.

Wendt, I., and C. Carl. 1991. “The statistical distribution of the mean squared weighted deviation.” *Chemical Geology: Isotope Geoscience Section* 86 (4): 275–85. [https://doi.org/10.1016/0168-9622\(91\)90010-t](https://doi.org/10.1016/0168-9622(91)90010-t).

Wetherill, George W. 1956. “Discordant uranium-lead ages, I.” *Eos, Transactions American Geophysical Union* 37 (3): 320–26. <https://doi.org/10.1029/tr037i003p00320>.